Journal of Materials Chemistry A

Accepted Manuscript

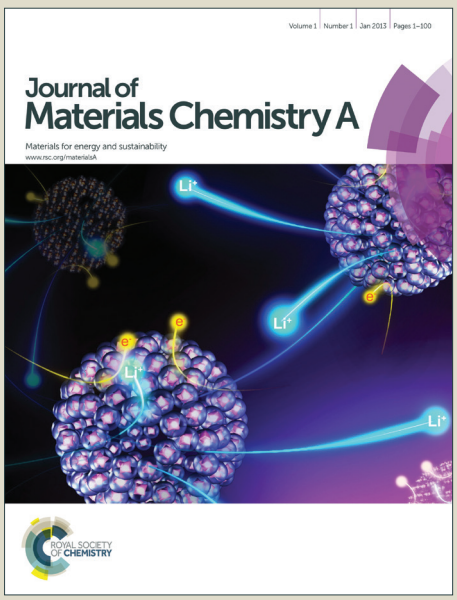

ROYAL SOCIETY OF CHEMISTRY

www.rsc.org/materialsA

Cite this: DOI: 10.1039/c0xx00000x

www.rsc.org/xxxxxx

ARTICLE TYPE

One-pot synthesis of core/shell Co@C spheres by catalytic carbonization of mixed plastics and their application in the photo-degradation of Cong red†

Jiang Gong[a,b], Jie Liu[a], Xuecheng Chen[a,c], Zhiwei Jiang[a,b], Xin Wen[a], Ewa Mijowska[c], Tao Tang*[a]

Received (in XXX, XXX) Xth XXXXXXXXX 200X, Accepted Xth XXXXXXXXX 200X
DOI: 10.1039/b000000x

Much attention has been paid to the synthesis of core/shell metal@carbon composites, but many of the proposed methods were limited in sophisticated procedure and expensive precursor. Herein, a facile one-pot approach was established to prepare magnetic core/shell Co@C spheres through catalytic carbonization of mixed plastics (consisting of polypropylene, polyethylene and polystyrene) by Co_3O_4 at 700 ^oC. The yield, composition, morphology, phase structure, textural property, surface element composition, thermal stability and magnetic property of core/shell Co@C spheres were investigated. The core/shell Co@C spheres had a distinct ordered and curved graphitic structure, and their main diameters were in the range of 110–130 nm. Besides, they showed a ferromagnetic behavior with high saturation magnetization (85.6–101.6 emu/g). Furthermore, it was observed that Co_3O_4 was uniformly distributed in mixed plastics and formed network structure, which provided a precondition for the carbonization of mixed plastics into core/shell Co@C spheres with uniform sizes. Finally, the core/shell Co@C spheres were found to show high performance in photo-degradation of Cong red (CR) with good recyclablity, reusability and long-term stability. It was demonstrated that the outer carbon shell promoted the degradation of CR and served as protective layer for cobalt core to improve acid resistance, while the inner cobalt core accelerated the decomposition of H_2O_2 into radicals, which catalyzed the degradation of CR. More importantly, this simple approach offers a potential way to prepare magnetic core/shell metal@carbon composites from cheap waste plastics.

1. Introduction

Recently, the core/shell carbon coated metal (metal@carbon) composites with their combined characters of carbon and metal materials have been a hot research topic in multifunctional composites.[1–6] This is ascribed to their broad range of potential applications in bioengineering materials,[7] catalysts,[8–10] environmental remediation,[10–16] and energy,[17] *etc*. Up to now, various methods have been developed for the synthesis of core/shell metal@carbon composites, for example, chemical vapor deposition (CVD),[6] pulsed plasma,[7] solvothermal method,[12] hydrothermal,[10,13] arc discharge,[18] pyrolysis,[19,20] high pressure CVD,[21] solid-state thermolysis,[22] thermal dissociation,[23] and detonation.[24–26] Various carbon-containing compounds are used as carbon sources such as methane,[6,27] ethanol,[7] polypyrrole,[9] glucose,[10,12] polyvinyl alcohol,[11] epoxy resin,[19] phenolic resin,[20] organometallic complex,[21–24] 1,3,5-trinitroperhydro-1,3,5-triazine,[25] acetylene,[27] CO,[28] and oleic acid.[29] However, many of these methods usually require high pressure, vacuum system, expensive or toxic precursor, organic solvent or sophisticated procedure, which limit their applications. Consequently, the development of cost-effective and environmentally friendly methods is highly desirable for the large-scale production and application of core/shell metal@carbon composites.

From a sustainable point of view, reutilization of plastics to synthesize core/shell metal@carbon composites not only shows advantages with cheap and abundant sources, but also provides a potential way to recycle waste plastics. This is because the total amount of waste plastics generated by human society is ever-increasing (*e.g.*, from 1.7 million tons in 1950 to 280 million tons in 2011[30]), and becoming a serious environmental problem. The tradition disposal ways of waste plastics are landfill and incineration, but they are far from being widely accepted by the population due to their related pollution problems. Upcycling plastics into carbon nanomaterials has been a novel method since most of plastics mainly conatin carbon element. Currently, most studies are focused on the production of carbon nanotubes (CNTs), carbon nanofibers (CNFs) and carbon spheres (CSs) from plastics. For example, Zhuo *et al*. reported the synthesis of CNTs from polyethylene (PE) using stainless-steel wire mesh as catalyst by a pyrolysis–combustion technique.[31] Pol *et al*. used autoclave as reactor to convert PE into CNTs under high pressure.[32] Our group found the combination of solid acid (or halogenated compound, or activated carbon) with nickel catalyst could effectively convert plastics into CNTs, CNFs and CSs

under atmospheric condition.[33–42]

Unfortunately, few studies are carried on to synthesize core/shell metal@carbon composites using plastics as carbon sources. Kong *et al.* synthesized Fe_3O_4@C composite through catalytic decomposition of PE in autoclave at 500 °C,[43] but the high pressure nature of autoclave was not in favor of massive and continuous production. Chen *et al.* prepared Co@C sphere using polypropylene (PP) as carbon source at 900 °C,[44] but the obtained Co@C sphere showed extreme heterogeneity in the size distribution and the yield was rather low (about 9 wt %). Zhu *et al.* reported the synthesis of Ni@C particle by pyrolyzing polystyrene (PS) using Ni@NiO particle as catalyst at 450 °C,[45] but the synthesized procedure was complicated and organic solvent-consuming. Additionally, the "real-world" waste plastics are actually mixture which is mainly composed of PP, PE and PS,[46] and to the best of our knowledge, there are no reports to prepare magnetic core/shell metal@carbon composites using mixed plastics as carbon sources. Consequently, an efficient strategy capable of producing magnetic core/shell metal@carbon composites in large scale from mixed plastics under mild condition is highly demanded.

Herein, a facile one-pot approach was established to synthesize uniform magnetic core/shell Co@C spheres through catalytic carbonization of mixed plastics (consisting of PP, PE and PS) using commercial Co_3O_4 as catalyst at 700 °C. Firstly, the yield, composition, morphology, microstructure, phase structure, textural property, surface element composition, thermal stability and magnetic property of core/shell Co@C spheres were investigated. Subsequently, a possible mechanism was put forward to explain the growth of magnetic core/shell Co@C spheres using mixed plastics as carbon sources. Finally, the resultant magnetic core/shell Co@C spheres were used for the photo-degradation of Congo red (CR), and the stability and reusability were explored. With simplicity, low cost in operation and easy availability of raw materials, this simple approach offers an opportunity for large-scale synthesis of magnetic core/shell metal@carbon composites using waste plastics as carbon sources.

2. Experiment part

2.1 Materials

Polypropylene (PP, weight-average molecular weight (M_w) = 3.07 × 10^5 g/mol, polydispersity index (PDI) = 3.13, and trademark T30S) powder was supplied by Yanan Petrochemical Co., China. High density polyethylene (PE, M_w = 1.53 × 10^5 g/mol, PDI = 5.55, and trademark 5306J) pellet was obtained from Sinopec Yangzi Petrochemical Co., Ltd, China. Polystyrene (PS, M_w = 3.72 × 10^5 g/mol, PDI = 1.78, and trademark PG-383) pellet was supplied by Zhenjiang Qimei Chemical Co., Ltd., China. Co_3O_4 was analytical-grade quality and purchased from Sinopharm Chemical Reagents Co., Ltd., China. Congo red (CR, supplied by Alfa Aesar) was of analytical-grade quality and used without further purification. All other chemicals were of analytical-grade quality.

2.2 Preparation of of samples

Mixed plastics consisting of PP (26.9 wt %, 9.42 g), PE (56.3 wt %, 19.70 g) and PS (16.8 wt %, 5.88 g) were mixed with a designed amount of Co_3O_4 in a Brabender mixer at 100 rpm and 180 °C for 10 min. The resultant sample was designed as polymer/Co_3O_4-x, where polymer and x represented the "mixed plastics" and the amount of Co_3O_4 (g/100g polymer), respectively.

2.3 Preparation of magnetic core/shell Co@C spheres

Magnetic core/shell Co@C spheres were prepared through carbonization experiment by heating polymer/Co_3O_4-x in a crucible at 700 °C according to our previous reports.[34,38] Briefly, a piece of polymer/Co_3O_4-x (about 11.0 g) was placed into a crucible, which was heated at 700 °C for about 6 min. After cooling down to room temperature, the resultant residue in the crucible was designated as Co@C-y, where y represented the amount of Co_3O_4 in the polymer/Co_3O_4-x (g/100g polymer). The yield of Co@C-y was calculated by dividing the amount of the residue by that of mixed plastics. Each measurement was repeated four times for the purpose of reproducibility.

2.4 Photo-degradation of CR using Co@C spheres

Co@C spheres were used for the photo-degradation of CR. The photochemical reactor was made of a Petri dish with diameter 105 mm and height 15 mm. An 8 W tubular UV lamp (from Spectronics Corporation, USA), which basically emits at 254 nm, was used as UV light source. The initial pH of CR solution was adjusted by 0.5 mol/L HCl solution. In a typical experiment, a solution of 50 mL containing CR (100 mg/L) and designed concentrations of Co@C-60 and H_2O_2 was mechanically stirred under UV irradiation. At given irradiation time intervals, 1.0 mL of solution was withdrawn by syringe, diluted, filtered through 0.45 μm membrane and immediately analyzed with UV/Vis/NIR spectrophotometer (Lambda 900). The degradation efficiency of CR was calculated by the following expression:

$$\text{Degradation efficiency of CR (\%)} = \frac{100\% * (C_0 - C_t)}{C_0}$$

where C_0 and C_t are the initial and t min concentration of CR (mg/L) in the solution, respectively.

2.5 Characterization

The morphology of Co@C-y was observed by field-emission scanning electron microscope (SEM, XL30ESEM-FEG). The microstructure of Co@C-y was investigated using transmission electron microscope (TEM, JEM-1011) at an accelerating voltage of 100 kV and high-resolution TEM (HRTEM) on a FEI Tecnai G2 S-Twin transmission electron microscope operating at 200 kV. The phase structure of Co@C-y was analyzed by X-ray diffraction (XRD) using a D8 advance X-ray diffractometer with Cu Kα radiation operating at 40 kV and 200 mA. Raman spectroscopy (T6400, excitation-beam wavelength: 514.5 nm) was used to characterize the vibrational property of Co@C-y. The textural property of Co@C-y was measured by N_2 sorption at 77 K using a Quantachrome Autosorb-1C-MS analyzer. The specific surface area was calculated by BET method, and the contribution of micropore to both volume and surface area was evaluated by means of the t-plot method. FT-IR spectrum was recorded on a Bio-Rad FTS 135 spectrophotometer. The content of Co element in the Co@C-y and in the solution after photo-degradation of CR was measured using inductively coupled plasma-optical omission spectrometer (ICP-OES, iCAP 6000 Series, Thermo Scientific).

The contents of C and H elements in the Co@C-y were measured by Elementar (Vario EL, Germany). The content of oxygen element in the Co@C-y was determined by the difference. The surface element composition of Co@C-y was characterized by X-ray photoelectron spectroscopy (XPS) carried out on a VG ESCALAB MK II spectrometer using an Al Kα exciting radiation from an X-ray source operated at 10.0 kV and 10 mA. The thermal stability of Co@C-y was measured by thermal gravimetric analysis (TGA) under air flow at a heating rate of 10 ^{o}C/min using a TA Instruments SDT Q600. The magnetic property of Co@C-y was carried out using a magnetic property measurement system (MPMS XL-7) at 300 K. The morphologies of mixed plastics and its mixture were observed by SEM (XL30ESEM-FEG). The rheological properties of mixed plastics and its mixture were conducted on a controlled strain rate rheometer (ARES rheometer) under nitrogen atmosphere. Round samples 25 mm (diameter) × 1 mm (thickness) were run at 180 °C. Frequency sweep was performed from 0.01 to 100 rad/s, with a strain of 1% in order to make the materials be in linear viscoelastic response.

3. Results and discussion

3.1 Morphology of Co@C spheres

Fig. 1 shows SEM images of the resultant Co@C spheres from polymer/Co_3O_4 at low and high magnifications. Clearly, a great amount of aggregated spherical-shape particles were observed in the resultant Co@C spheres. Upon amplification, the spherical particles could be clearly seen with diameters in the range of 80−150 nm. When the content of Co_3O_4 catalyst was increased, the size of Co@C spheres did not show obvious changes. The microstructure of Co@C spheres was studied by TEM observation. As shown in Fig. 2, the Co@C spheres exhibited the desirable core/shell structure with carbon coated on metallic cobalt core. Although these particles looked locally agglomerated, because the particle-to-particle distances were very small, the boundary of each particle was clearly visible. The diameter distributions of core/shell Co@C spheres were shown in Fig. S1 in ESI †. The average diameter was calculated to be 120 ± 17 nm for Co@C-10, 126 ± 14 nm for Co@C-20, 125 ± 22 nm for Co@C-30, 122 ± 17 nm for Co@C-40, 122 ± 16 nm for Co@C-50, and 118 ± 16 nm for Co@C-60. Hence, the content of Co_3O_4 did not influence the diameter of core/shell Co@C spheres.

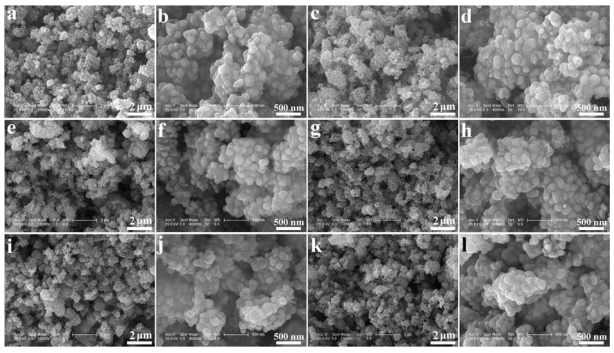

Fig. 1 Typical SEM images of Co@C spheres from polymer/Co_3O_4: (a and b) Co@C-10, (c and d) Co@C-20, (e and f) Co@C-30, (g and h) Co@C-40, (i and j) Co@C-50, and (k and l) Co@C-60.

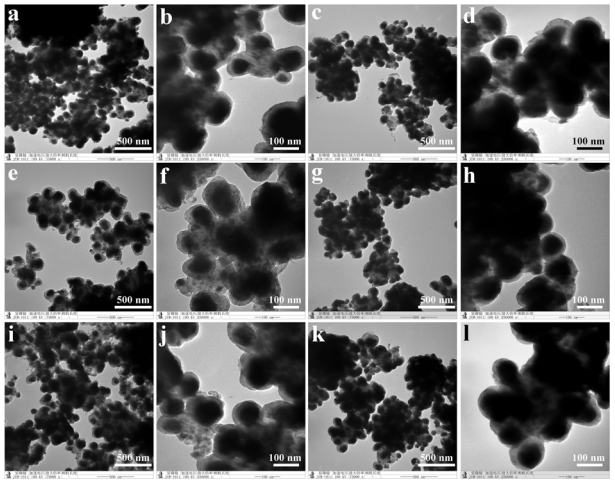

Fig. 2 Typical TEM images of Co@C spheres from polymer/Co_3O_4: (a and b) Co@C-10, (c and d) Co@C-20, (e and f) Co@C-30, (g and h) Co@C-40, (i and j) Co@C-50, and (k and l) Co@C-60.

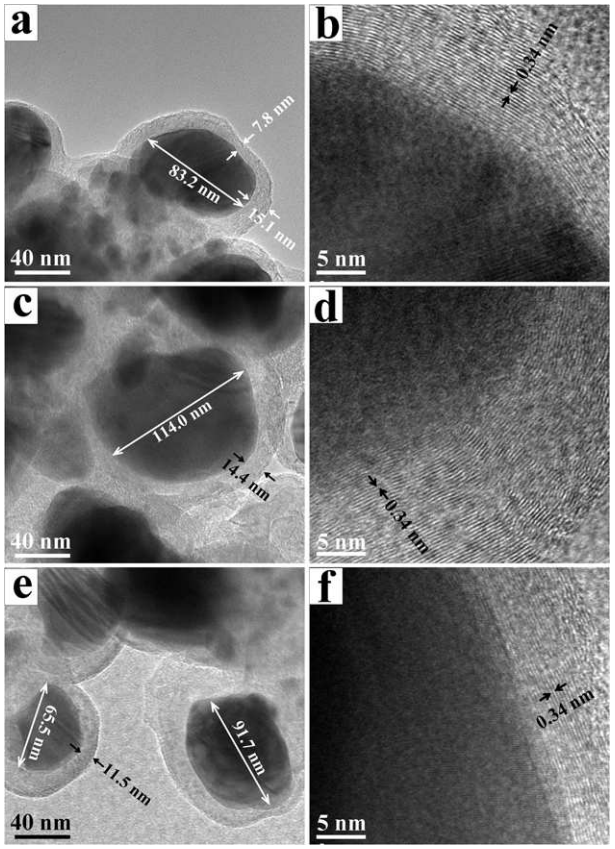

Fig. 3 HRTEM images of core/shell Co@C spheres from polymer/Co_3O_4: (a and b) Co@C-10, (c and d) Co@C-30, and (e and f) Co@C-60.

In addition, the concentrations of other forms of carbon such as rods, fibers and tubes were negligible. To gain more detailed information about the internal microstructure of core/shell Co@C spheres, HRTEM observations were conducted on the Co@C-10, Co@C-30 and Co@C-60, which confirmed the core/shell

microstructure (Fig. 3). Obviously, the carbon shell had a distinct ordered and curved graphitic structure, and the interlayer spacing between graphitic layers was about 0.34 nm, consistent with the ideal graphitic interlayer spacing. The thicknesses of graphitic shells fell in the range of 4−16 nm, while the main diameters of cobalt particles were between 65 and 130 nm.

3.2 Yield, carbon conversion, composition and surface element composition of core/shell Co@C spheres

Table 1 presents the yield of core/shell Co@C spheres from catalytic carbonization of mixed plastics by Co_3O_4 at 700 °C. Notably, it increased from 10.9 to 42.0 wt %, when the content of Co_3O_4 was increased from 10 to 60 (g/100g polymer). Meanwhile, the carbon conversion of mixed plastics was increased from 5.4 to 26.7 wt %, suggesting that Co_3O_4 promoted the carbonization of mixed plastics. The element composition of core/shell Co@C spheres was measured by ICP-OES and elemental analysis (Table 1). The results indicated that Co@C spheres consisted of carbon, cobalt, hydrogen and oxygen elements. The contents of carbon and cobalt elements were in the ranges of 32.3−39.2 wt % and 50.4−56.3 wt %, respectively. The presence of oxygen element (5.9−10.8 wt %) probably resulted from the oxidation during the carbonization and/or the cooling process.

Table 1 Yield, carbon conversion and composition of core/shell Co@C spheres.

Sample	Yield [a] (wt %)	Conversion [b] (wt %)	Content of element (wt %)			
			C [c]	Co [d]	H [c]	O [e]
Co@C-10	10.9	5.4	38.0	55.9	0.3	5.9
Co@C-20	18.1	8.1	32.3	54.3	0.2	13.2
Co@C-30	27.6	15.9	38.0	51.0	0.1	10.8
Co@C-40	33.1	19.5	37.4	53.3	0.1	9.2
Co@C-50	39.0	25.1	39.2	50.4	0.1	10.3
Co@C-60	42.0	26.7	34.8	56.3	0.1	8.7

[a] Calculated by dividing the amount of core/shell Co@C spheres (*i.e.*, the residue in the crucible) by that of polymer/Co_3O_4 in the crucible. [b] Calculated by dividing the amount of carbon in the obtained core/shell Co@C spheres by that of carbon element in the polymer/Co_3O_4. [c] Calculated by elemental analysis. [d] Calculated by ICP-OES. [e] Calculated by the difference.

XPS measurement was used to characterize the surface element composition of the core/shell Co@C spheres (Fig. 4). It revealed that the surface of core/shell Co@C spheres mainly consisted of C (83.5–97.1 at %) and O (2.4–16.4 at %) elements with a trace amount of Co element (0.1–0.8 at %). To determine the chemical component and the oxidation state of C element, high-resolution XPS spectra of C_{1s} were curve-fitted into four individual peaks: graphitic carbon (284.4–284.6 eV), C–OH (285.6–285.8 eV), C=O (286.9–287.1 eV) and COOH (288.9–289.1 eV) (Fig. 5). As a consequence, the carbon element on the surface of core/shell Co@C spheres existed mainly in the presence of graphitic carbon with relatively small amounts of C–OH, C=O and COOH. The surface functional groups could contribute to the removal of heavy metallic ions[12] or organic dyes[13] when the core/shell Co@C spheres were used as adsorbents in wastewater treatment.

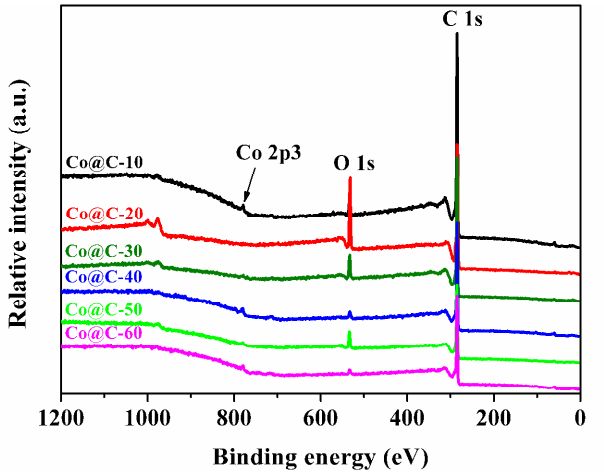

Fig. 4 XPS patterns of core/shell Co@C spheres.

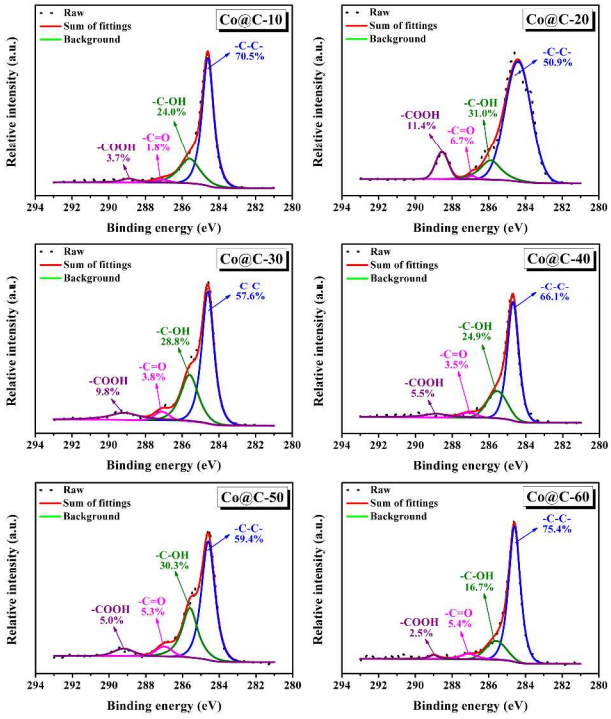

Fig. 5 C1s high-resolution XPS spectra of core/shell Co@C spheres.

3.3 Phase structure, textural property, thermal stability and magnetic property of core/shell Co@C spheres

Fig. 6a displays the XRD patterns of the core/shell Co@C spheres and polymer/Co_3O_4-60. Compared to the XRD pattern of polymer/Co_3O_4-60, the diffraction peaks of mixed plastics (2θ = 15–25°) and Co_3O_4 (2θ = 19.2° (111), 31.5° (220), 37.1° (311), 38.8° (222), 45.1° (400), 45.9° (422), 59.6° (511), 65.5° (440),

74.4° (620), 77.6° (533), 78.6° (622) and 82.8° (444)) disappeared completely after the carbonization, meanwhile the diffraction peaks of face-centered cubic metallic cobalt (2θ = 44.8° (111), 52.0° (200) and 76.3° (220)) appeared obviously. This implied that Co_3O_4 was reduced into metallic cobalt during the carbonization. The encapsulating carbon was also observed as a very weak peak around 26.2° (002). Fig. 6b shows the Raman spectra of the obtained core/shell Co@C spheres. The peak at about 1580 cm^{-1} (G band) corresponds to an E_{2g} mode of hexagonal graphite and is related to the vibration of sp^2-bonded carbon atoms in a graphite layer. This meant that the core/shell Co@C spheres were composed of graphitic carbon, consistent with HRTEM result (Fig. 3). The D band at about 1350 cm^{-1} is associated with the vibration of carbon atoms with dangling bonds in the plane terminations of disordered graphite. The intensity ratio of G band and D band (I_G/I_D ratio) provides information about the crystallinity of core/shell Co@C spheres.[47] The I_G/I_D ratio was in the range of 0.50–0.54, reflecting the presence of a relative high amount of disordered carbon in the core/shell Co@C spheres.

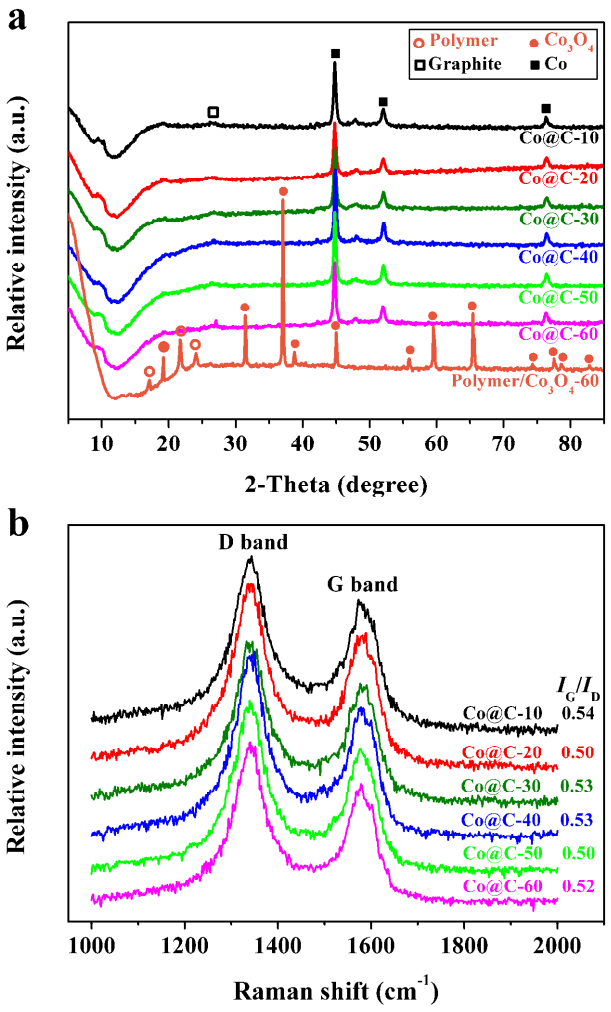

Fig. 6 XRD patterns (a) of core/shell Co@C spheres and polymer/Co_3O_4-60, and Raman spectra (b) of core/shell Co@C spheres.

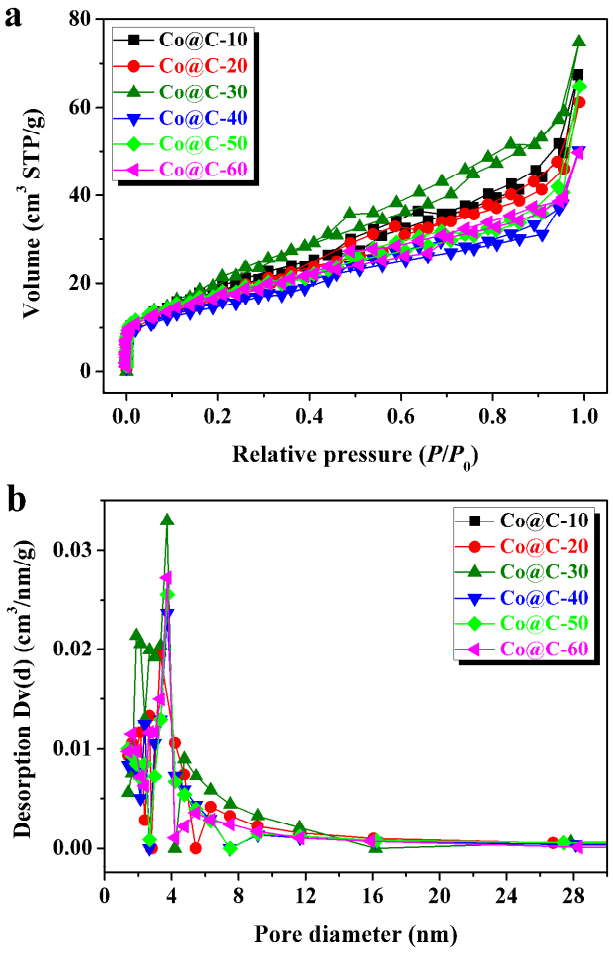

Fig. 7 Nitrogen adsorption–desorption isotherms (a) and pore size distributions (b) of core/shell Co@C spheres.

Table 2 Textural parameters of core/shell Co@C spheres.

Property	Co@C-y (y = 10–60)					
	10	20	30	40	50	60
S_{BET} (m^2/g) [a]	71.2	67.0	82.7	55.4	62.4	62.0
S_{micro} (m^2/g) [b]	13.7	9.3	1.2	1.4	11.3	14.6
S_{meso} (m^2/g) [c]	57.5	57.7	81.5	54.0	51.1	47.4
V_{total} (cm^3/g) [d]	0.10	0.10	0.12	0.08	0.10	0.08
V_{micro} (cm^3/g) [e]	0.01	0.01	0.00	0.00	0.01	0.01
V_{meso} (cm^3/g) [f]	0.09	0.09	0.12	0.08	0.09	0.07
D_{AV} (nm) [g]	3.74	3.31	3.73	3.74	3.74	3.74

[a] The total specific surface area. [b] The specific surface area of micropores. [c] The specific surface area of mesopores. [d] The total volume. [e] The volume of micropores. [f] The volume of mesopores. [g] The average diameter of pores.

The N_2 adsorption-desorption isotherms of core/shell Co@C spheres (Fig. 7a) showed the type-IV curve and exhibited a hysteresis loop associated to capillary condensation in the range

of P/P_0 being from 0.5 to 1.0. This indicated that the porosity of the core/shell Co@C spheres was essentially made up of mesopores. The textural properties of core/shell Co@C spheres, including BET surface area (S_{BET}), micropore surface area (S_{micro}), mesopore surface area (S_{meso}), total pore volume (V_{total}), micropore volume (V_{micro}), mesopore volume (V_{meso}) and average pore diameter (D_{AV}), are summarized in Table 2. S_{BET}, S_{meso}, V_{total} and V_{meso} of core/shell Co@C spheres were in the ranges of 55.4–82.7 m^2/g, 47.4–81.5 m^2/g, 0.08–0.12 cm^3/g and 0.07–0.12 cm^3/g, respectively. The pore size distributions of core/shell Co@C spheres were calculated using the Barrett–Joyner–Halenda (BJH) model from the desorption branches of the isotherms (Fig. 7b). This clearly showed that the size of mesopores in the core/shell Co@C spheres was in the narrow range of 2–8 nm (centered on 3.7 nm). The mesopores could be attributed to the cavities in the carbon shell.

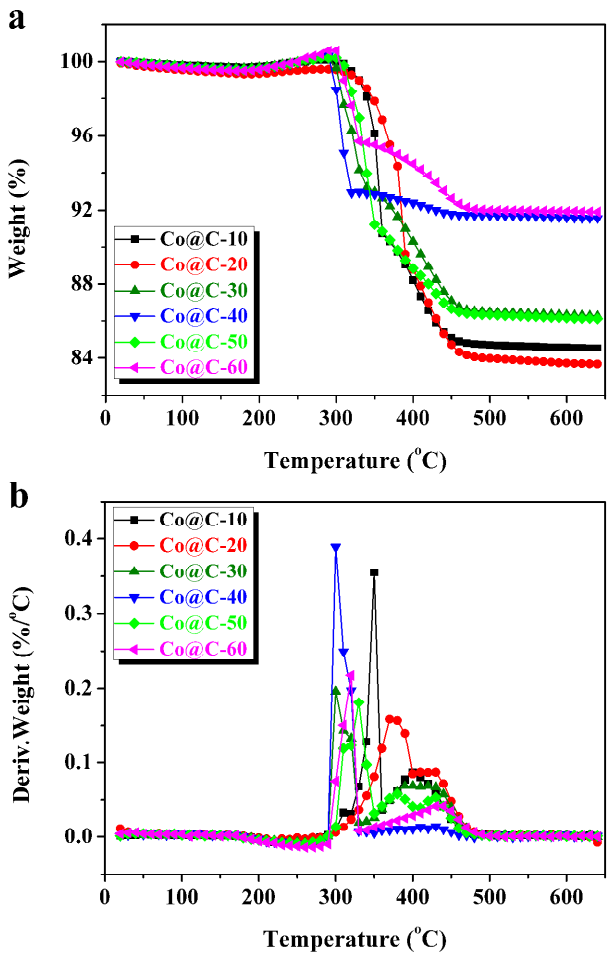

Fig. 8 TGA (a) and DTG (b) curves of core/shell Co@C spheres under air flow at 10 °C/min.

TGA and the derivative TGA (DTG) were used to evaluate the thermal stability of core/shell Co@C spheres (Fig. 8). The weight loss before 100 °C was due to the evaporation of physically adsorbed water molecules. The second weak region of weight increase from 100 to 300 °C was attributed to the release of chemisorbed water, pyrolysis of oxygen containing functional groups and oxidation of metallic cobalt into Co_2O_3. A remarkable weight loss occurred between 300 and 650 °C, ascribed to the oxidation degradation of carbon skeleton of graphite shells and the oxidation of metallic cobalt into Co_2O_3. The residue of Co@C-y (y = 10, 20, 30, 40, 50 and 60) at 650 °C was 84.5, 83.7, 86.3, 91.6, 86.1 and 91.9%, respectively, therefore, the content of metallic cobalt in the Co@C-y was calculated to be 60.0, 59.5, 61.3, 65.1, 61.2 and 65.3%, respectively, since metallic cobalt was oxidized into Co_2O_3. These results were approximate to those calculated by ICP-OES (Table 1).

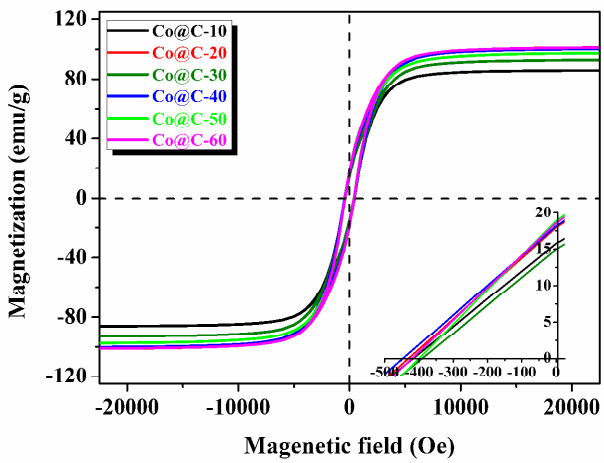

Fig. 9 The magnetic property of core/shell Co@C spheres. The magnetic hysteresis loops measured by MPMS XL-7.

Table 3 Magnetic parameters of core/shell Co@C spheres according to Fig. 9.

Sample	M_S[a] (emu/g)	M_R[b] (emu/g)	M_S/M_R	M_C[c] (Oe)
Co@C-10	85.6	15.8	0.18	416.6
Co@C-20	101.6	18.0	0.18	430.0
Co@C-30	92.9	15.0	0.16	390.4
Co@C-40	100.4	18.2	0.18	446.4
Co@C-50	97.9	18.9	0.19	400.0
Co@C-60	101.3	18.6	0.18	419.5

[a] The saturation magnetization. [b] The remanent magnetization. [c] The coercivity.

Magnetic property of the core/shell Co@C spheres is measured by MPMS XL-7 at 300 K and displayed by magnetization hysteresis loops in Fig. 9. The magnetic parameters of core/shell Co@C spheres are listed in Table 3. For all Co@C spheres, the data implied a ferromagnetic behavior as indicated by the open hysteresis loops. The quantitative analysis yielded the saturation magnetization (M_s) of 85.6–101.6 emu/g, demonstrating that the core/shell Co@C spheres possessed a strong response to an external magnet. The M_s value was much higher than that from other reports such as 0.3 emu/g,[44] 1.14

emu/g,[48] and 35.7 emu/g.[7] The remanent magnetization values (M_R) amounted to 15.8–18.9 emu/g. The ratio of M_R/M_S was in the range of 0.16–0.19, confirming the ferromagnetic behavior of core/shell Co@C spheres at the room temperature. The coercivity (M_C) was between 390.4 and 446.4 Oe. Overall, these magnetic data showed the suitability of core/shell Co@C spheres for potential applications in magnetic recording materials, cancer treatment, drug delivery and magnetic resonance imaging, *etc*.

3.4 Discussion about the growth mechanism of magnetic core/shell Co@C spheres

To study the growth mechanism of magnetic core/shell Co@C spheres, the dispersion state of Co_3O_4 in the mixed plastics is observed by SEM and the results are displayed in Fig. 10. It was observed that PS was immiscible with PP and PE, and existed in the form of microspheres (Fig. 10a), while Co_3O_4 catalyst with a size range of 100–400 nm (detected as white dots) was uniformly distributed in PP/PE (Fig. 10b). More Co_3O_4 particles were observed in PP/PE when the content of Co_3O_4 catalyst was increased to 30 or 60 wt % (Figs. 10c and 10d), however, the size of Co_3O_4 particles did not show obvious changes. This was probably ascribed to the formation of Co_3O_4 network in the mixed plastics, which was demonstrated by the change of dynamic melt rheological property of polymer (*i.e.*, the mixed plastics) and polymer/Co_3O_4-x. The storage modulus (G') in the low frequency (ω) regime is significantly dependent on the addition of Co_3O_4. The rheological property in the low ω regime reflects the relaxation and motion of the whole polymer chains.[49] Fig. 11 shows the G'–ω curves of polymer and polymer/Co_3O_4-x at 180 °C. It was observed that the terminal slope of G'-ω curve decreased compared with that of mixed plastics when 10 wt % Co_3O_4 was added, and G'-ω curve exhibited a distinct plateau at the low ω when 60 wt % Co_3O_4 was added. This result demonstrated a transition from liquid-like state to solid-like state due to the formation of Co_3O_4 network structure in the mixed plastics.

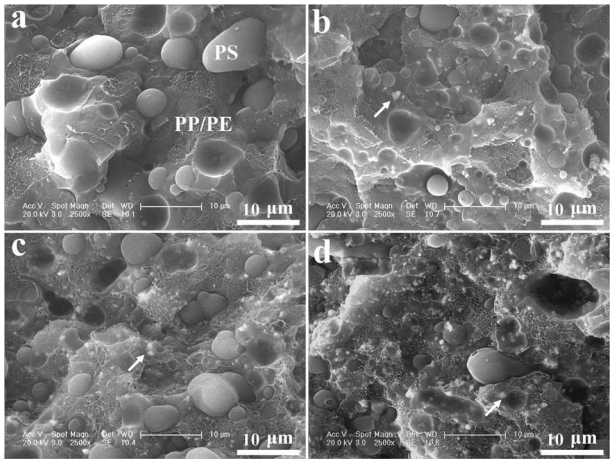

Fig. 10 Typical SEM images of polymer (*i.e.*, the mixed plastics) (a), polymer/Co_3O_4-10 (b), polymer/Co_3O_4-30 (c), and polymer/Co_3O_4-60 (d).

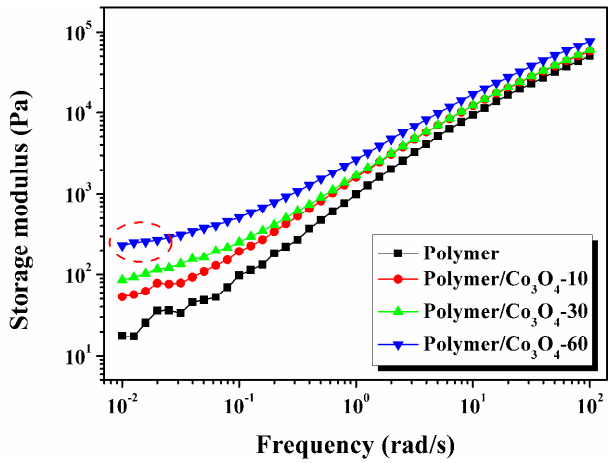

Fig. 11 Storage modulus of polymer, polymer/Co_3O_4-10, polymer/Co_3O_4-30 and polymer/Co_3O_4-60.

Based on the above results, the formation mechanism of magnetic core/shell Co@C spheres through catalytic carbonization of mixed PP, PE and PS by Co_3O_4 at 700 °C was put forward (Fig. 12). Firstly, Co_3O_4 was uniformly dispersed in the mixed plastics by melt mixing (Fig. 12a). Subsequently, the mixed plastics were pyrolyzed into light hydrocarbons and aromatics under high temperature[36,37] (Fig. 12b). The resultant light hydrocarbons and aromatics were dehydrogenated and aromatizated on the surface of Co_3O_4 catalyst,[41] meanwhile Co_3O_4 was reduced into metallic cobalt, which has some (about 1 at %) carbon solubility in the solid solution.[50] After further carbonization of degradation products, once supersaturated, carbon precipitated from the surface of metallic cobalt particles to form core/shell Co@C spheres (Fig. 12c). Obviously, the dispersion of Co_3O_4 particles in the mixed plastics played an important role in the formation of uniform core/shell Co@C spheres, and the metallic cobalt particles from the reduction of Co_3O_4 acted as templates for the growth of carbon shells.

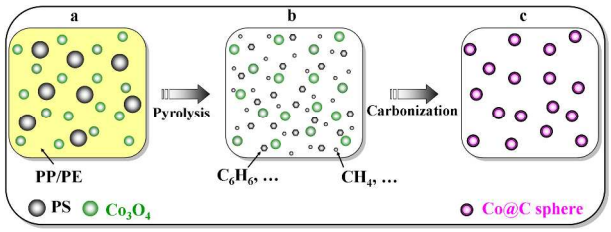

Fig. 12 Mechanism about the formation of core/shell Co@C spheres through catalytic carbonization of mixed PP, PE and PS by Co_3O_4.

3.5 Photo-degradation of CR using Co@C spheres

To study the photo-degradation of CR, Co@C-60 was firstly selected as an example since the yield of Co@C-60 was the highest (Table 1). Fig. 13 shows the degradation behavior of CR under different experimental conditions. As can be seen, CR is rather stable under UV irradaitaion. Only slight color removal of CR (5.3%) was observed after UV irradiation for 180 min in the system containing H_2O_2. This suggested that few hydroxyl radicals (·OH) were formed by the decomposition of H_2O_2

without Co@C-60.[51] For UV + Co@C-60 system, 15.6% degradation efficiency of CR was obtained after UV irradiation for 180 min, approximate to Dark + Co@C-60 system (14.5%), indicating that the photo-activity of Co@C-60 was so poor in the absence of H_2O_2. For H_2O_2 + Co@C-60 system, the degradation efficiency of CR (35.0%) was enhanced due to the combined effect of Co@C-60 and H_2O_2 in the absence of UV irradiation. Comparatively, UV irradiation further accelerated the photo-degradation of CR in the H_2O_2 + Co@C-60 system. 98.1% photo-degradation efficiency of CR was observed after 180 min UV irradiation. To gain a deeper insight into the reaction mechanism, 2-propanol, a typical hydroxyl radicals scavenger,[52] was used to investigate the catalytic performance of Co@C-60 sphere. In the presence of 2-propanol, the UV + H_2O_2 + Co@C-60 system gave 16.1% degradation efficiency of CR, which was much lower than that in the absence of 2-propanol (98.1%) and nearly equivalent to that in the UV + Co@C-60 system (15.6%). This implied that the catalytic degradation of CR in 2-propanol was likely to involve predominant hydroxyl radicals, because the introduction of 2-propanol could lead to an obvious decrease of catalytic activity in the system based on hydroxyl radicals. Additionally, the photo-degradation efficiency of CR in the UV + H_2O_2 + Co@C-y (y = 10, 20, 30, 40, 50) system was 98.6%, 99.1%, 98.9%, 98.5% and 99.0%, repectively.

To study the role of carbon shell in the degradation of CR, carbon sphere (C-60) was obtained by immersing Co@C-60 in 12 M HCl aqueous solution at room temperature for three months to remove cobalt core. The degradation efficiency of CR in UV + C-60 system was about 10.7%, approximate to UV + Co@C-60 and UV + H_2O_2 + C-60 systems. Hence, carbon shell of Co@C-60 had a certain adsorption capacity of CR from the bulk solution, which could be further demonstrated by the FT-IR results (Fig. S2). A similar phenomenon was observed by Kojin et al.[14] They found that carbon coating could accelerate the photo-degradation of pollutants by concentrating pollutants around $W_{18}O_{49}$ crystal *via* adsorption.

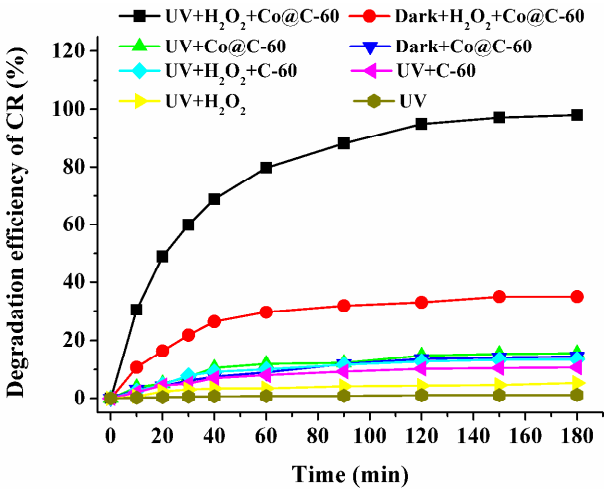

Fig. 13 The degradation behavior of CR under different experimental conditions. Experimental conditions: Co@C-60 dosage = 1.0 g/L or C-60 dosage = 0.35 g/L, initial CR concentration = 100 mg/L, initial H_2O_2 concentration = 43.6 mM, and pH = 3.

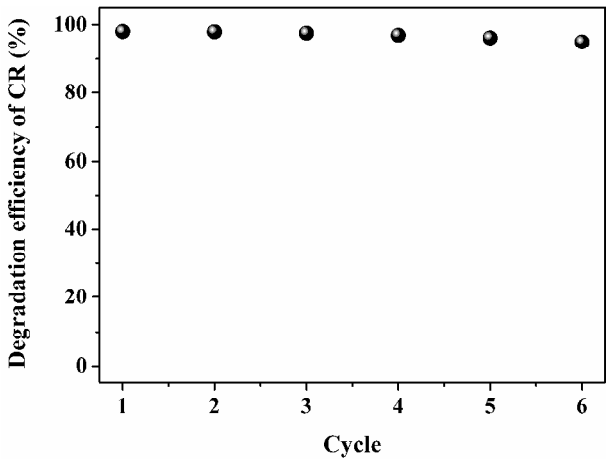

Fig. 14 The reusability of core/shell Co@C-60 sphere for the photo-degradation of CR. Experimental conditions: Co@C-60 dosage = 1.0 g/L, initial CR concentration = 100 mg/L, initial H_2O_2 concentration = 43.6 mM, pH = 3, and UV irradiation time = 180 min.

As well known, one severe problem that magnetic materials faced is the stability in the acid environment. To make materials have real-life applications, the anti-acid ability of core/shell Co@C spheres is needed to be investigated. 0.8 g core/shell Co@C-60 sphere was added into 12 M HCl acid solution (100 mL) at room temperature. Even after four weeks, the Co@C-60 sphere still exhibited magnetically responsive property (Fig. S3). In fact, it needed at least three months to remove completely the cobalt core. The excellent anti-acid ability of core/shell Co@C spheres was mainly ascribed to the protection by the outer carbon shell. As a result, the outer carbon shell not only promoted the degradation of CR, but also served as protective layer for the cobalt core to improve acid resistance.

The recyclablity and reusability of core/shell Co@C spheres are very important to its practical application. One of the advantages using core/shell Co@C spheres is that they can be separated by a magnet due to their high M_s (Table 3). To study the reusability, the recycled Co@C-60 is reused for six cycles, and the results of the photo-degradation of CR are shown in Figs. 14 and S4. After six cycles, the photo-degradation efficiency of CR was as high as 95.0%, and the morphology of Co@C-60 did not change after the photo-catalytic reactions. In previous studies,[53–55] it was demonstrated that the cobalt^{2+}-bicarbonate complex accelerated the decomposition of H_2O_2 into radicals (such as ·OH), which catalyzed the degradation of organic dyes. Similarly, in this work, we speculated that the dissolved Co^{2+} in the solution (about 0.9 ppm measured by ICP-OES) played an important role in the decomposition of H_2O_2 into radicals, which promoted the degradation of CR. Overall, the core/shell Co@C spheres showed high performance in the photo-degradation of CR with good recyclablity, reusability and long-term stability. Further investigations about the effects of various influencing factors such as the dosage of core/shell Co@C spheres, initial CR concentration, initial H_2O_2 concentration and pH of CR solution on the photo-degradation efficiency of CR are on the way in our laboratory to better understand the photo-degradation property of the magnetic core/shell Co@C spheres.

Conclusions

Magnetic core/shell Co@C spheres were effectively synthesized *via* a novel one-pot approach through catalytic carbonization of mixed PP/PE/PS by Co_3O_4. The core/shell Co@C spheres had a distinct ordered and curved graphitic structure. They showed a ferromagnetic behavior and had high saturation magnetization. It was found that the good distribution of Co_3O_4 in the mixed plastics provided a precondition for the formation of uniform core/shell Co@C spheres. Furthermore, the core/shell Co@C spheres showed high performance in the photo-degradation of CR with good recyclablity, reusability and long-term stability, indicating that they had the potential application in the wastewater treatment. It is believed, with simplicity, low cost in operation and easy availability of raw materials, this simple approach opens up a new avenue in large-scale synthesis of functional core/shell metal@carbon composites using waste plastics as carbon sources.

Acknowledgements

We would like to thank the reviewers for kind and important suggestions. This work was supported by the National Natural Science Foundation of China (51373171, 2124079, 51233005 and 21374114) and Polish Foundation (No. 2011/03/D/ST5/06119).

Notes and references

[a] *State Key Laboratory of Polymer Physics and Chemistry, Changchun Institute of Applied Chemistry, Chinese Academy of Sciences, Changchun 130022, China. Fax: +86 (0) 431 85262827; Tel: +86 (0) 431 85262004; E-mail: ttang@ciac.ac.cn*

[b] *University of Chinese Academy of Sciences, Beijing 100049, China*

[c] *Institute of Chemical and Environment Engineering, West Pomeranian University of Technology, Szczecinul. Pulaskiego 10, 70-322 Szczecin, Poland*

† Electronic Supplementary Information (ESI) available: The diameter distribution of core/shell Co@C spheres; FT-IR spetra; photograph showing the Co@C-60 attracted by a magnet after being soaked in 12 M HCl solution for four weeks; the CR degradation curves during different cycles.

References

1 S. Y. Wei, Q. Wang, J. H. Zhu, L. Y. Sun, H. F. Lin and Z. H. Guo, *Nanoscale*, 2011, **3**, 4474.
2 Y. P. Zhai, Y. Q. Dou, X. X. Liu, B. Tu and D. Y. Zhao, *J. Mater. Chem.*, 2009, **19**, 3292.
3 Q. F. Liu, Z. G. Chen, B. L. Liu, W. C. Ren, F. Li, H. T. Cong and H. M. Cheng, *Carbon*, 2008, **46**, 1892.
4 M. M. Titirici and M. Antonietti, *Chem. Soc. Rev.*, 2010, **39**, 103.
5 B. Hu, K. Wang, L. H. Wu, S. H. Yu, M. Antonietti and M. M. Titirici, *Adv. Mater.*, 2010, **22**, 813.
6 J. S. Qiu, Q. X. Li, Z. Y. Wang, Y. F. Sun and H. Z. Zhang, *Carbon*, 2006, **44**, 2565.
7 Z. Abdullaeva, E. Omurzak, C. Iwamoto, H. S. Ganapathy, S. Sulaimankulova, C. Liliang and T. Mashimo, *Carbon*, 2012, **50**, 1776.
8 C. G. Tan and R. N. Grass, *Chem. Commun.*, 2008, 4297.
9 T. J. Yao, T. Y. Cui, J. Wu, Q. Z. Chen, X. J. Yin, F. Cui and K. N. Sun, *Carbon*, 2012, **50**, 2287.
10 M. Y. Zhu, C. J. Wang, D. H. Meng and G. W. Diao, *J. Mater. Chem. A*, 2013, **1**, 2118.
11 D. Zhang, S. Y. Wei, C. Kaila, X. Su, J. Wu, A. B. Karki, D. P. Young and Z. H. Guo, *Nanoscale*, 2010, **2**, 917.
12 J. Zheng, Z. Q. Liu, X. S. Zhao, M. Liu, X. Liu and W. Chu, *Nanotechnology*, 2012, **23**, 165601.
13 Z. Y. Zhang and J. L. Kong, *J. Hazard. Mater.*, 2011, **193**, 325.
14 F. Kojin, M. Mori, Y. Noda and M. Inagaki, *Appl. Catal. B: Environ.*, 2008, **78**, 202.
15 H. Sun, G. Zhou, S. Liu, H. M. Ang, M. O. Tadé and S.Wang, *ACS Appl. Mater. Interfaces*, 2012, **4**, 6235.
16 P. Zhang, C. Shao, M. Zhang, Z. Guo, J. Mu, Z. Zhang, X. Zhang, P. Liang and Y. Liu, *J. Hazard. Mater.*, 2012, **229–230**, 265.
17 W. M. Zhang, X. L. Wu, J. S. Hu, Y. G. Guo and L. J. Wan, *Adv. Funct. Mater.*, 2008, **18**, 3941.
18 B. S. Xu, J. J. Guo, X. M. Wang, X. G. Liu and H. Ichinose, *Carbon*, 2006, **44**, 2631.
19 J. H. Zhu, S. Pallavkar, M. J. Chen, N. Yerra, Z. P. Luo, H. A. Colorado, H. F. Lin, N. Haldolaarachchige, A. Khasanov, T. C. Ho, D. P. Young, S. Y. Wei and Z. H. Guo, *Chem. Commun.*, 2013, **49**, 258.
20 Y. A. Huang, Z. Xu, Y. Yang, T. Tang, R. S. Huang and J. Y. Shen, *J. Phys. Chem. C*, 2009, **113**, 6533.
21 A. A. El-Gendy, E. M. M. Ibrahim1, V. O. Khavrus, Y. Krupskaya, S. Hampel, A. Leonhardt, B. Büchner and R. Klingeler, *Carbon*, 2009, **47**, 2821.
22 B. E. Hamaoui, L. J. Zhi, J. S. Wu, U. Kolb and K. Müllen, *Adv. Mater.*, 2005, **17**, 2957.
23 S. V. Pol, V. G. Pol, A. Frydman, G. N. Churilov and A. Gedanken, *J. Phys. Chem. B*, 2005, **109**, 9495.
24 G. L. Sun, X. J. Li, Y. J. Zhang, X. H. Wang, D. A. Jiang and F. Mo, *J. Alloy. Compd.*, 2009, **437**, 212.
25 N. Luo, K. X. Liu, Z. Y. Liu, X. J. Li, S. Y. Chen, Y. Shen and T. W. Chen, *Nanotechnology*, 2012, **23**, 475603.
26 N. Luo, X. Li, X. Wang, H. Yan, F. Mo, W. Sun, *Compos. Sci. Technol.*, 2009, **69**, 2554.
27 M. Bystrzejewski, A. Huczko, H. Lange, P. Baranowski, G. Cota-Sanchez, G. Soucy, J. Szczytko and A. Twardowski, *Nanotechnology*, 2007, **18**, 145608.
28 W. M. Zhu, J. W. Ren, X. Gu, M. U. Azmat, G. Z. Lu and Y. Q. Wang, *Carbon*, 2011, **48**, 1462.
29 V. Sunny, D. S. Kumar, Y. Yoshida, M. Makarewicz, W. Tabiś and M. R. Anantharaman, *Carbon*, 2010, **48**, 1643.
30 C. W. Zhuo and Y. A. Levendis, *J. Appl. Polym. Sci.*, 2014, **131**, 39931.
31 C. W. Zhuo, B. Hall, H. Richter and Y. Levendis, *Carbon*, 2010, **48**, 4024.
32 V. G. Pol and M. M. Thackeray, *Energy Environ. Sci.*, 2011, **4**, 1904.
33 T. Tang, X. C. Chen, X. Y. Meng, H. Chen and Y. P. Ding, *Angew. Chem. Int. Ed.*, 2005, **44**, 1517.
34 Z. W. Jiang, R. J. Song, W. G. Bi, J. Lu and T. Tang, *Carbon*, 2007, **45**, 449.
35 R. J. Song, Z. W. Jiang, W. G. Bi, W. X. Cheng, J. Lu, B. T. Huang and T. Tang, *Chem. Eur. J.*, 2007, **13**, 3234.
36 J. Gong, J. Liu, Z. W. Jiang, X. Wen, X. C. Chen, E. Mijowska, Y. H. Wang and T. Tang, *Chem. Eng. J.*, 2013, **225**, 798.
37 J. Gong, J. D. Feng, J. Liu, R. Muhammad, X. C. Chen, Z. W. Jiang, E. Mijowska, X. Wen and T. Tang, *Ind. Eng. Chem. Res.*, 2013, **52**, 15578.
38 J. Gong, J. Liu, L. Ma, X. Wen, X. C. Chen, D. Wan, H. O. Yu, Z. W. Jiang, E. Borowiak-Palen and T. Tang, *Appl. Catal. B: Environ.*, 2012, **117–118**, 185.
39 J. Gong, K. Yao, J. Liu, X. Wen, X. C. Chen, Z. W. Jiang, E. Mijowska and T. Tang, *Chem. Eng. J.*, 2013, **215–216**, 339.
40 J. Gong, J. Liu, Z. W. Jiang, J. D. Feng, X. C. Chen, L. Wang, E. Mijowska, X. Wen and T. Tang, *Appl. Catal. B: Environ.*, 2014, **147,** 592.
41 J. Gong, J. Liu, D. Wan, X. C. Chen, X. Wen, E. Mijowska, Z. W. Jiang, Y. H. Wang and T. Tang, *Appl. Catal. A: Gen.*, 2012, **449**, 112.
42 J. Gong, J. Liu, X. C. Chen, X. Wen, Z. W. Jiang, E. Mijowska, Y. H. Wang and T. Tang, *Micropor. Mesopor. Mater.*, 2013, **176**, 31.
43 J. H. Zhang, B. Yan, S. Wan and Q. H. Kong, *Ind. Eng. Chem. Res.*, 2013, **52**, 5708.
44 X. C. Chen, H. Wang and J. H. He, *Nanotechnology*, 2008, **19**, 325607.

45 J. H. Zhu, S. Y. Wei, Y. F. Li, S. Pallavkar, H. F. Lin, N. Haldolaarachchige, Z. P. Luo, D. P. Young and Z. H. Guo, *J. Mater. Chem.*, 2011, **21**, 16239.
46 C. F. Wu and P. T. Williams, *Fuel*, 2010, **89**, 3022.
47 J. O. Alves, C. W. Zhuo, Y. A. Levendis and J. A. S. Tenório, *Appl. Catal. B: Environ.*, 2011, **106**, 433.
48 C. Yu and J. S. Qiu, *Chem. Eng. Res. Des.*, 2008, **86**, 904.
49 H. O. Yu, J. Liu, Z. Wang, Z. W. Jiang and T. Tang, *J. Phys. Chem. C*, 2009, **113**, 13092.
50 C. P. Deck and K.Vecchio, *Carbon*, 2006, **44**, 267.
51 J. Gong, K. Yao, J. Liu, Z. W. Jiang, X. C. Chen, X. Wen, E. Mijowska, N. N. Tian and T. Tang, *J. Mater. Chem. A*, 2013, **1**, 5247.
52 M. Mrowetz and E. Selli, *Phys. Chem. Chem. Phys.*, 2005, **7**, 1100.
53 A. H. Xu, X. X. Li, S. Ye, G. C. Yin and Q. F. Zeng, *Appl. Catal. B: Environ.*, 2011, **102**, 37.
54 Z. Yang, H. Wang, M. Chen, M. X. Luo, D. S. Xia, A. H. Xu and Q. F. Zeng, *Ind. Eng. Chem. Res.*, 2012, **51**, 11104.
55 X. X. Li, Z. D. Xiong, X. C. Ruan, D. S. Xia, Q. F. Zeng and A. H. Xu, *Appl. Catal. A: Gen.*, 2012, **411–412**, 24.

Table of Contents (TOC)

One-pot synthesis of core/shell Co@C spheres by catalytic carbonization of mixed plastics and their application in the photo-degradation of Cong red

Jiang Gong, Jie Liu, Xuecheng Chen, Zhiwei Jiang, Xin Wen, Ewa Mijowska, Tao Tang*

Co_3O_4 catalyzed carbonization of plastics into Co@C spheres *via* a one-pot approach, which showed high performance in photo-degradation of CR.